Synthesis, Structure, and Reactivity of Nitrosyl Pincer-Type Rhodium Complexes

Carina Gaviglio,[†] Yehoshoa Ben-David,[‡] Linda J. W. Shimon,[#] Fabio Doctorovich,[†] and David Milstein*[,‡]

Department of Organic Chemistry and Department of Chemical Research Support, The Weizmann Institute of Science, Rehovot, 76100, Israel, and Departamento de Química Inorgánica, Analítica y Química Física/INQUIMAE-CONICET, Facultad de Ciencias Exactas y Naturales, Universidad de Buenos Aires, Ciudad Universitaria, Pabellón II, Piso 3, (C1428EHA) Buenos Aires, Argentina

Received December 4, 2008

Pincer-type linear nitrosyl Rh(I) complexes, Rh(PCP^{t}Bu)(NO)][BF_4] (**2**) and [Rh(PCP^{t}BuCH$_2$)(NO)][BF_4] (**8**), are reported (PCP^{t}Bu = 1,3-bis[(di-*tert*-butylphosphino)methyl]-2,4,6-trimethylbenzene). Complex **2** was synthesized by reaction of the Rh(I) dinitrogen complex Rh(PCP^{t}Bu)N_2 (**1**) with $NOBF_4$, while treatment of the methyl chloride complex Rh(PCP^{t}Bu)(CH_3)Cl (**7**) with $NOBF_4$ led to the formation of **8**. Upon addition of CO, a linear ↔ bent nitrosyl equilibrium was established, both in solution and in the solid state, between the linear nitrosyl Rh(I) complex **2** and the bent nitrosyl Rh(III) complex [Rh(PCP^{t}Bu)(NO)(CO)][BF_4] (**3**). Addition of LiCl to complex **2** resulted in the quantitative formation of the bent nitrosyl complex Rh(PCP^{t}Bu)(NO)(Cl) (**4**). An IR study of solvent interactions of the nitrosyl ligand of complex **2** in various solvents is also presented, showing a linear ↔ bent nitrosyl equilibrium induced by solvent coordination. Treatment of **4** with $HBF_4 \cdot O(C_2H_5)_2$ led to chloride abstraction, with formation of complex **2**. Upon addition of $NOBF_4$ to the PNP Rh(I) complex [$C_5H_3N(CH_2P(^tBu)_2)_2Rh(CH_3CN)$][$BF_4$] (**5**), the bent nitrosyl complex [$C_5H_3N(CH_2P(^tBu)_2)_2Rh(CH_3CN)(NO)$][$BF_4$]$_2$ (**6**) was obtained. Employing ^{15}NO-labeled complexes it is possible to assign the bent or linear modes of bonding of NO on the basis of ^{15}N NMR spectroscopy. X-ray structures of all nitrosyl complexes reported here confirm that the tetracoordinate species are square-planar with a linear nitrosyl ligand occupying the position *trans* to the aromatic ring and the metal is Rh(I), whereas the pentacoordinate complexes adopt a square-pyramidal geometry with a bent apical nitrosyl coordinated to Rh(III).

Introduction

For many years, much attention has been focused on synthetic, structural, and spectroscopic aspects of transition metal nitrosyl complexes, as well as on the reactivity of the coordinated NO moiety, motivated by the fundamental role of NO in biochemical systems and in coordination chemistry.[1] The ability of the NO ligand to coordinate to transition metal complexes in either a nearly linear or bent fashion is well known. The linear arrangement has been viewed in terms of an NO^+ ligand and the bent arrangement in terms of NO^-.[1,2] The interconversion of bent and linear nitrosyls formally leads to a change in metal oxidation state, $M^{z+}(NO)^+ \leftrightarrow M^{(z+2)+}(NO)^-$, maintaining in this way the total number of electrons "*n*", denoted with a classically rationalized description as {MNO}^{n}, where "*n*" stands for the number of electrons associated with the metal d and π^*_{NO} orbitals.[3,4] This change in electronic distribution is generally accompanied by a change in the coordination geometry, which may constitute the basis for catalytic reactions.[1,5] Therefore, reactions of nitrosyl transition metal complexes are interesting in their own right and because of their relevance to catalysis and to biochemical processes.[1,6]

Pincer-type complexes play an important role in transition metal chemistry, enhancing the stability of complexes and allowing the use of steric and electronic parameters that moderate reactivity at the metal center. Late transition metal complexes of bulky PCP-type pincer ligands have found applications in synthesis, bond activation, and catalysis.[7] Complexes of the ligand PCP^{t}Bu (PCP^{t}Bu = 1,3-bis[(di-*tert*-butylphosphino)methyl]-2,4,6-trimethylbenzene)[8] have been utilized in various catalytic applications. Among these are the iridium(I)-catalyzed alkane dehydrogenation reactions and C−C bond-forming reactions.[7i,9] In addition, PNP^{t}Bu-type complexes (PNP^{t}Bu = 2,6-bis(di-*tert*-butylphosphinomethyl)pyridine)[10] have also shown interesting reactivity, such as the selective

* Corresponding author. E-mail: david.milstein@weizmann.ac.il.
‡ Department of Organic Chemistry, The Weizmann Institute of Science.
# Department of Chemical Research Support, The Weizmann Institute of Science.
† Universidad de Buenos Aires.

(1) (a) Machura, B. *Coord. Chem. Rev.* **2005**, *249*, 2277–2307. (b) Coppens, P.; Novozhilova, I.; Kovalevsky, A. *Chem. Rev.* **2002**, *102*, 861–884. (c) Roncaroli, F.; Videla, M.; Slep, L. D.; Olabe, J. A. *Coord. Chem. Rev.* **2007**, *251*, 1903–1930.

(2) Richter-Addo, G. B.; Legzdins, P. *Metals Nitrosyls*; Oxford University Press: New York, 1992.

(3) (a) Enemark, J. H.; Feltham, R. D. *Coord. Chem. Rev.* **1974**, *13*, 339–406. (b) Enemark, J. H.; Feltham, R. D. *Top. Stereochem.* **1981**, *12*, 155–215.

(4) For early examples of equilibria between linear and bent nitrosyl complexes, see: (a) Pratt Brock, C.; Collman, J. P.; Dolcetti, G.; Farnham, P. h.; Ibers, J. A.; Lester, J. E.; Reed, C. A. *Inorg. Chem.* **1973**, *12*, 1304–1313. (b) Schoonover, M. W.; Baker, E. C.; Eisenberg, R. *J. Am. Chem. Soc.* **1979**, *101*, 1880–1882. (c) Mason, J.; Mingos, D. M. P.; Sherman, D.; Wardle, R. W. M. *J. Chem. Soc., Chem. Commun.* **1984**, *122*, 3–1225.

(5) Hayton, W. T.; Legzdins, P.; Sharp, W. B. *Chem. Rev.* **2002**, *102*, 935–991.

(6) (a) McCleverty, J. A. *Chem. Rev.* **2004**, *104*, 403–418. (b) Miranda, K. M. *Coord. Chem. Rev.* **2005**, *249*, 433–455.

10.1021/om8011536 CCC: $40.75
Publication on Web 02/25/2009

activation of the *ortho* C−H bonds of haloarenes[11] and the sp^3 C−H bonds of ketones at the β-position by the complex [(PNP^{t}Bu)Ir(COE)][BF_4] (COE = cyclooctene).[12] This complex also exhibits metal−ligand cooperation in C−H and H_2 activation involving facile ligand dearomatization−aromatization.[13] Dehydrogenation alcohols[14] as well as H/D exchange of aromatic C−H bonds with D_2O or C_6D_6[15] are efficiently catalyzed by PNP^{t}Bu-Ru complexes.

Herein, we report the synthesis of {RhNO}^{8} nitrosyl complexes with PCP^{t}Bu and PNP^{t}Bu pincer-type ligands. Complete spectroscopic and structural characterization is presented, and their reactivity toward CO, LiCl, and $HBF_4 \cdot O(C_2H_5)_2$ is reported. Solvent interactions with the nitrosyl ligand were also studied.

Results and Discussion

Synthesis of a Linear Nitrosyl Rh(I) Phosphine Complex (2). To the best of our knowledge, no pincer PCP-type rhodium nitrosyl complexes are known. A PNP rhodium bent nitrosyl complex was reported.[16a] Linear nitrosyl complexes of rhenium with pincer-type PNP ligands were recently published.[17] Reaction of the Rh(I) complex Rh(PCP^{t}Bu)N_2[18] (**1**) with 1 equiv of $NOBF_4$ resulted in substitution of the N_2 ligand and formation of the novel nitrosyl Rh(I) phosphine complex [Rh(PCP^{t}Bu)(NO)][BF_4] (**2**) (Scheme 1).

Complex **2** was fully characterized by multinuclear NMR techniques, IR, X-ray diffraction, and elemental analysis. The

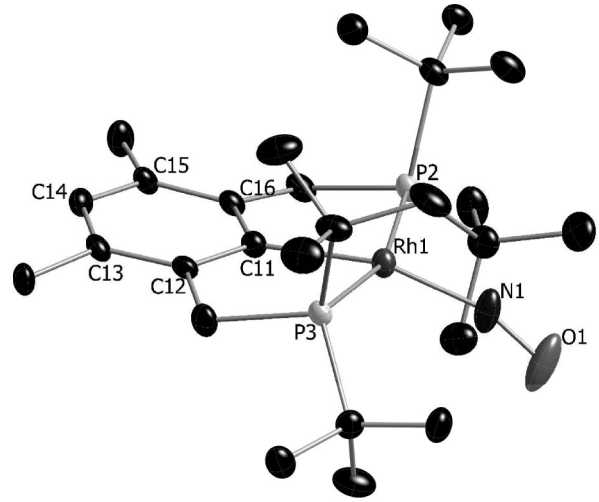

Figure 1. ORTEP plot of complex **2** at the 50% probability level. Hydrogen atoms and counteranion are omitted for clarity.

Scheme 1

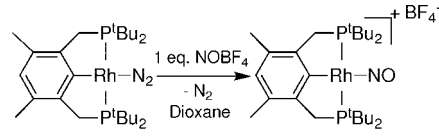

1 **2**

$^{31}P\{^1H\}$ NMR spectrum of **2** exhibits a doublet at δ 104.02 with a $^1J_{Rh,P}$ of 130.6 Hz, indicative of two chemically equivalent phosphorus nuclei coordinated to a Rh(I) center. In the ^{15}N NMR spectrum the signal due to the ^{15}N-enriched nitrosyl complex **2** appears at δ 377.88 ppm as a doublet with a $^1J_{Rh,N}$ of 35.5 Hz, characteristic of a bound linear nitrosyl.[19] In CH_2Cl_2 solution the complex exhibits a strong band in the IR spectrum at 1834 cm^{-1}, and in the solid state a strong split band characteristic of a ν(NO) stretching vibration at 1841, 1817 cm^{-1} is observed.[20] The assignment of this band to the NO ligand was confirmed by use of the ^{15}N-labeled derivative [Rh(PCP^{t}Bu)(^{15}NO)][BF_4], with a frequency at 1802, 1777 cm^{-1}. These data are consistent with a linear nitrosyl.[19]

The molecular structure of **2** was confirmed by an X-ray diffraction study of single crystals obtained by slow diffusion of pentane into a concentrated solution of **2** in CH_2Cl_2 at room temperature (Figure 1).

The rhodium atom is located in the center of a square-planar geometry with the nitrosyl group occupying the position *trans* to the *ipso* carbon. The N−O bond distance of 1.175(7) Å and the Rh−N−O angle of 159.9(6)° are in the range expected for a linear nitrosyl in analogous systems.[17] Choualeb et al. reported a N−O bond distance of 1.223(6) Å and a Re−N−O angle of 171.8(5)° for the linear nitrosyl rhenium complex with a pincer-type PNP ligand, ReHBr(NO)[HN(C_2H_4P^{t}Bu$_2$)$_2$].[17] Deviation from linearity of the nitrosyl ligand in complex **2** is probably a result of strong σ-donation of the aryl ring.[21] Relevant structural parameters of complex **2** are shown in Table 1.

(7) Reviews: (a) Pugh, D.; Danopoulos, A. A. *Coord. Chem. Rev.* **2007**, *251*, 610–641. (b) Szabó, K. J. *Synlett* **2006**, *6*, 811–824. (c) Rybtchinski, B.; Milstein, D. *ACS Symp. Ser.* **2004**, *885*, 70–85. (d) van der Boom, M. E.; Milstein, D. *Chem. Rev.* **2003**, *103*, 1759–1792. (e) Singleton, J. T. *Tetrahedron* **2003**, *59*, 1837–1857. (f) Milstein, D. *Pure Appl. Chem.* **2003**, *75*, 445–460. (g) Albrecht, M.; van Koten, G. *Angew. Chem., Int. Ed.* **2001**, *40*, 3750–3781. (h) Vigalok, A.; Milstein, D. *Acc. Chem. Res.* **2001**, *34*, 798–807. (i) Jensen, C. M. *Chem. Commun.* **1999**, 2443–2449. (j) Rybtchinski, B.; Milstein, D. *Angew. Chem., Int. Ed.* **1999**, *38*, 870–883.

(8) Rybtchinsky, B.; Vigalok, A.; Ben-David, Y.; Milstein, D. *J. Am. Chem. Soc.* **1996**, *118*, 12406–12415.

(9) (a) Gupta, M.; Hagen, C.; Flesher, R.; Kaska, W. C.; Jensen, C. M. *Chem. Commun.* **1996**, 2083. (b) Xu, W. W.; Rosini, G. P.; Krogh-Jespersen, K.; Goldman, A. S.; Gupta, M.; Jensen, C. M.; Kaska, W. C. *Chem. Commun.* **1997**, 2273–2274. (c) Liu, F.; Goldman, A. S. *Chem. Commun.* **1999**, 655. (d) Renkema, K. B.; Kissin, Y. V.; Goldman, A. S. *J. Am. Chem. Soc.* **2003**, *125*, 7770. (e) Morales-Morales, D.; Lee, D. W.; Wang, Z.; Jensen, C. M. *Organometallics* **2001**, *20*, 1144. (f) Haenel, M. W.; Oevers, S.; Angermund, K.; Kaska, W. C.; Fan, H. J.; Hall, M. B. *Angew. Chem.* **2001**, *113*, 3708; *Angew. Chem., Int. Ed.* **2001**, *40*, 3596. (g) Gottker-Schnetmann, I.; White, P. S.; Brookhart, M. *J. Am. Chem. Soc.* **2004**, *126*, 1804.

(10) Hermann, D.; Gandelman, M.; Rozenberg, H.; Shimon, L. J. W.; Milstein, D. *Organometallics* **2002**, *21*, 812–818.

(11) (a) Ben-Ari, E.; Gandelman, M.; Rozenberg, H.; Shimon, L. J. W.; Milstein, D. *J. Am. Chem. Soc.* **2003**, *125*, 4714–4715. (b) Ben-Ari, E.; Gandelman, M.; Shimon, L. J. W.; Martin, J. M. L.; Milstein, D. *Organometallics* **2006**, *25*, 3190–3210.

(12) Feller, M.; Karton, A.; Leitus, G.; Martin, J. M. L.; Milstein, D. *J. Am. Chem. Soc.* **2006**, *128*, 12400–12401.

(13) Ben-Ari, E.; Leitus, G.; Schimon, L. J. W.; Milstein, D. *J. Am. Chem. Soc.* **2006**, *128*, 15390–15391.

(14) (a) Zhang, J.; Gandelman, M.; Shimon, L. J. W.; Milstein, D. *Organometallics* **2004**, *23*, 4026–4033. (b) Zhang, J.; Leitus, G.; Ben-David, Y.; Milstein, D. *J. Am. Chem. Soc.* **2005**, *127*, 10840–10841.

(15) Prechtl, M. H. G.; Hölscher, M.; Ben-David, Y.; Theyssen, N.; Loschen, R.; Milstein, D.; Leitner, W. *Angew. Chem., Int. Ed.* **2007**, *46*, 2269–2272.

(16) (a) Feller, M.; Ben-Ari, E.; Gupta, T.; Shimon, L. J. W.; Leitus, G.; Diskin-Posner, Y.; Weiner, L.; Milstein, D. *Inorg. Chem.* **2007**, *46*, 10479–10490. (b) Böttcher, K.; Mereiter, K. *Inorg. Chem. Commun.* **2004**, *7*, 1225–1228. (c) Kelly, B. A.; Welch, A. J.; Woodward, P. *J. Chem. Soc., Dalton Trans.* **1977**, 2237. (d) Goldberg, S. Z.; Kubiak, C.; Meyer, C. D.; Eisenberg, R. *Inorg. Chem.* **1975**, *14*, 1650–1654.

(17) Choualeb, A.; Lough, A. J.; Gusev, S. G. *Organometallics* **2007**, *26*, 3509–3515.

(18) Vigalok, A.; Milstein, D. *Organometallics* **2000**, *19*, 2061–2064.

(19) (a) Bell, L. K.; Mason, J.; Mingos, D. M. P.; Tew, D. G. *Inorg. Chem.* **1983**, *22*, 3497–3502. (b) Mason, J.; Larkworthy, L. F.; Moore, E. A. *Chem. Rev.* **2002**, *102*, 913–934.

(20) The two bands are a solid state effect, as only one band is observed in solution (see Table 4). Note that the linear nitrosyl $CoCl_2(NO)(PMePh_2)_2$ was reported to be partially transformed to the bent nitrosyl isomer by grinding in preparation for a Nujol mull, resulting in two IR absorption bands: see ref 4a.

(21) Richter-Addo, G. B.; Wheeler, R. A.; Hixson, C. A.; Chen, L.; Khan, M. A.; Ellison, M. K.; Schulz, C. E.; Scheidt, R. *J. Am. Chem. Soc.* **2001**, *123*, 6314–6326.

Table 1. Selected Bond Lengths (Å) and Angles (deg) for 2

Rh(1)−N(1)	1.763(5)	C(11)−C(12)	1.421(7)
Rh(1)−C(11)	2.085(6)	C(12)−C(13)	1.397(7)
Rh(1)−P(2)	2.3443(15)	C(13)−C(14)	1.384(8)
Rh(1)−P(3)	2.3391(15)	C(14)−C(15)	1.404(7)
N(1)−O(1)	1.175(7)	C(15)−C(16)	1.400(7)
		C(16)−C(11)	1.418(7)
Rh(1)−N(1)−O(1)	159.9(6)	P(2)−Rh(1)−P(3)	162.32(4)
N(1)−Rh(1)−C(11)	161.6(2)	P(2)−Rh(1)−C(11)	82.08(16)
N(1)−Rh(1)−P(2)	98.98(17)	P(3)−Rh(1)−C(11)	82.18(16)
N(1)−Rh(1)−P(3)	98.50(17)		

Scheme 2

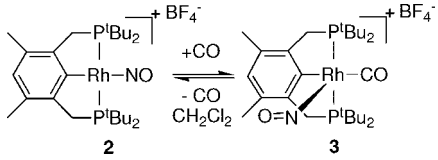

2 **3**

Reaction of Complex 2 with CO in CD_2Cl_2. Formation of [Rh(PCP^{t}Bu)(NO)(CO)][BF_4] (3). Upon treatment of a methylene chloride solution containing the nitrosyl Rh(I) complex **2** with 1 equiv of CO at room temperature, immediate and quantitative formation of complex **3** took place (Scheme 2).

The new pentacoordinate CO adduct **3** is stable in solution at low temperature, but at room temperature it is stable only under an excess of CO. The reaction appears to be reversible, with complex **2** being recovered from a methylene chloride solution of **3** upon standing at room temperature or upon evaporation of the methylene chloride solution of **3** under vacuum. A facile and well-defined linear ↔ bent nitrosyl equilibrium took place. The iridium complex [Ir(NO)(η^3-C_3H_5)(PPh_3)$_2$]$^+$ also exhibits in solution a linear−bent NO interchange, which occurs without an accompanying $\eta^3-\eta^1$ allyl fluxionality.[4b]

The $^{31}P\{^1H\}$ NMR spectrum of complex **3** gives rise to a doublet at δ 91.27 with a $^1J_{Rh,P}$ of 128.5 Hz, indicating two equivalent phosphorus nuclei coordinated to a Rh(III) center. The CO ligand appears in the $^{13}C\{^1H\}$ NMR spectrum as a double triplet at δ 189.55 with $^1J_{Rh,C} = 47.3$ Hz and $^2J_{PC} = 9.7$ Hz. The IR spectrum of **3** in CH_2Cl_2 solution shows a strong band at 2080, 2065 cm^{-1} (slightly split) assigned to ν(CO), while ν(NO) appears at 1699 cm^{-1}. The observed lower frequency of this complex in comparison to **2** is indicative of a bound bent NO.[19] The ^{15}N NMR spectrum of the ^{15}N-enriched nitrosyl complex **3** shows a broad singlet with a rather low-field resonance at δ 837.14 ppm, clearly assignable to the bent nitrosyl ligand, as already observed with other square-pyramidal {RhNO}^{8} nitrosyl complexes.[19] The dichloromethane-soluble complex **3** was crystallized from a concentrated dichloromethane solution at −30 °C. The X-ray structure revealed a square-pyramidal geometry with a bent apical nitrosyl ligand *trans* to the vacant coordination site and the CO ligand *trans* to the *ipso* carbon (Figure 2).

The Rh−N−O angle is 122.5(6)°, characteristic of bent NO,[16] while the N−O bond length is 1.158(10) Å, shorter in comparison to the linear nitrosyl complex **2** (N−O bond length 1.175(7) Å), probably due to the presence of the strongly π-accepting CO ligand (Table 2).

Thus, a linear-to-bent NO conformation change may be induced chemically by the addition of a neutral ligand such as CO to the metal center. Also, a temperature effect was observed; at low temperature the pentacoordinate CO adduct **3** was favored, while at room temperature the tetracoordinate complex **2** is preferred, resulting in a formal modulation of the oxidation state of the metal center from Rh(III) to Rh(I), respectively. The temperature dependence is expected based on entropy considerations.

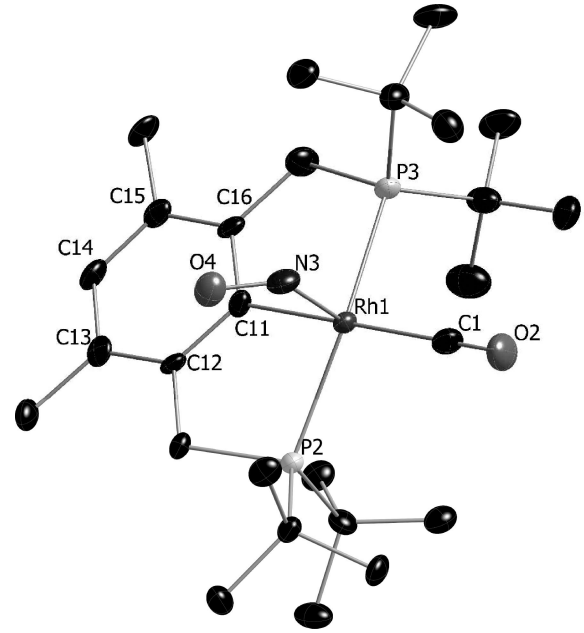

Figure 2. ORTEP plot of complex **3** at the 50% probability level. Hydrogen atoms and counteranion are omitted for clarity.

Table 2. Selected Bond Lengths (Å) and Angles (deg) for 3

Rh(1)−N(3)	1.975(8)	C(11)−C(12)	1.404(13)
Rh(1)−C(1)	1.985(10)	C(12)−C(13)	1.414(12)
Rh(1)−C(11)	2.092(8)	C(13)−C(14)	1.401(13)
Rh(1)−P(2)	2.352(2)	C(14)−C(15)	1.388(14)
Rh(1)−P(3)	2.383(2)	C(15)−C(16)	1.410(12)
N(4)−O(3)	1.158(10)	C(16)−C(11)	1.413(12)
C(1)−O(2)	1.119(12)		
Rh(1)−N(3)−O(4)	122.5(6)	P(2)−Rh(1)−C(11)	81.3(3)
N(3)−Rh(1)−C(1)	88.9(4)	P(3)−Rh(1)−C(11)	82.4(3)
N(3)−Rh(1)−P(3)	98.7(2)	C(1)−Rh(1)−C(11)	177.9(4)
N(3)−Rh(1)−P(2)	98.3(2)	C(1)−Rh(1)−P(2)	98.7(3)
N(3)−Rh(1)−C(11)	93.2(3)	C(1)−Rh(1)−P(3)	96.9(3)
P(2)−Rh(1)−P(3)	157.06(8)	Rh(1)−C(1)−O(2)	175.8(10)

Reaction of Complex 2 with $CO_{(g)}$ in the Solid State. Formation of [Rh(PCP^{t}Bu)(NO)(CO)][BF_4] (3). Quantitative formation of the pentacoordinate CO adduct **3** was also observed after addition of $CO_{(g)}$ to **2** in the solid state. As was observed in solution, an equilibrium reaction is also established between both species in the solid state, depending on the temperature and on the presence of excess $CO_{(g)}$. The stabilization of complex **3** is favored at low temperature, or at room temperature under a CO atmosphere. IR of the solid shows strong, sharp bands characteristic of ν(CO) at 2087, 2071 cm^{-1} (slightly split), and the ν(NO) stretching vibration appears at 1686 cm^{-1}. The assignment of this characteristic band to the NO ligand was confirmed by IR measurement of the ^{15}N-labeled derivative [Rh(PCP^{t}Bu)(^{15}NO)(CO)][BF_4], which gives rise to ν(NO) =1653 cm^{-1}.

Reaction of Complex 2 with LiCl. Formation of Rh(PCP^{t}Bu)(NO)(Cl) (4). Treatment of complex **2** with excess LiCl led to the nucleophilic attack of Cl^- on the metal center, resulting in selective formation of **4** as a single new product (Scheme 3).

The $^{31}P\{^1H\}$ NMR spectrum of **4** shows a doublet at δ 74.93, ca. 30 ppm upfield from that observed for the cationic complex **2**, with $^1J_{Rh,P} = 143.9$ Hz, indicating two equivalent phosphorus nuclei coordinated to a Rh(III) center. The IR spectrum displays

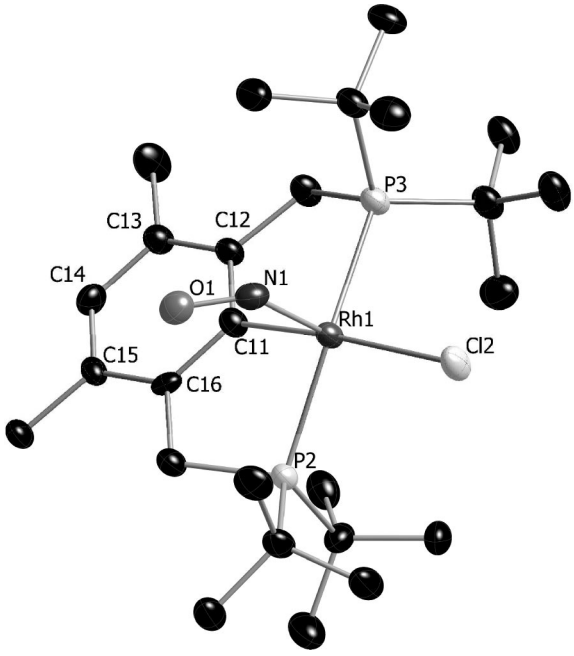

Figure 3. ORTEP plot of complex **4** at the 50% probability level. Hydrogen atoms are omitted for clarity.

Scheme 3

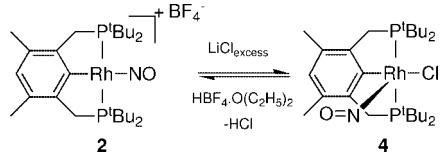

2 **4**

Table 3. Selected Bond Lengths (Å) and Angles (deg) for 4

Rh(1)−N(1)	1.890(3)	C(11)−C(12)	1.410(5)
Rh(1)−C(11)	2.059(4)	C(12)−C(13)	1.399(5)
Rh(1)−Cl(2)	2.465(1)	C(13)−C(14)	1.401(5)
Rh(1)−P(2)	2.313(1)	C(14)−C(15)	1.378(5)
Rh(1)−P(3)	2.382(1)	C(15)−C(16)	1.410(5)
N(1)−O(1)	1.184(4)	C(16)−C(11)	1.407(5)
Rh(1)−N(1)−O(1)	127.4(3)	P(2)−Rh(1)−C(11)	81.61(11)
N(1)−Rh(1)−Cl(2)	98.39(10)	P(3)−Rh(1)−C(11)	82.57(11)
N(1)−Rh(1)−P(3)	99.87(10)	Cl(2)−Rh(1)−C(11)	171.42(11)
N(1)−Rh(1)−P(2)	97.87(10)	Cl(2)−Rh(1)−P(2)	94.96(3)
N(1)−Rh(1)−C(11)	89.90(14)	Cl(2)−Rh(1)−P(3)	98.11(3)
P(2)−Rh(1)−P(3)	156.12(4)		

a diagnostic signal for bent NO at 1618 cm^{-1}. The assignment of this band to the nitrosyl ligand was confirmed by the ^{15}N-enriched nitrosyl complex **4**, which exhibited $\nu(NO) = 1585$ cm^{-1}. Also, ^{15}N NMR spectroscopy confirmed the presence of the bent nitrosyl in the ^{15}N-enriched nitrosyl complex **4**, showing a signal at δ 841.18 ppm as a broad singlet. Crystals of **4** suitable for X-ray analysis were grown from a concentrated solution of **4** in ether at −30 °C (Figure 3).

As in the case of complex **3**, the rhodium atom is located in the center of a square-pyramid with the bent apical nitrosyl group occupying the position *trans* to the empty coordination site and the Cl ligand *trans* to the aromatic ring. The Rh−N−O angle of 127.4(3)° confirms that NO is bent. The Rh−N bond distance is 1.890(3) Å and the N−O bond distance is 1.184(4) Å (Table 3). Comparing these bond distances with those of complex **3** (1.975(8) and 1.158(10) Å, respectively), we can observe that in complex **3** there is less back-bonding to the nitrosyl ligand than in complex **4**, probably due to the presence of the strong π-acceptor CO ligand in **3** and its cationic nature.

Table 4. IR Frequencies of the NO Ligand in Complex 2 in Various Solvents

solvent	ν_{NO} (cm^{-1})	*Z*	AN	DN	polarity
CH_2Cl_2	1834	64.2	20.4	1.6	0.726
CH_3CN	1714	71.3	18.9	14.1	0.924
CH_3OH	1709	83.6	41.3	19.1	0.914
DMSO	1662	71.1	19.3	29.8	0.938
pyridine	1645	64	14.2	33.1	
DMF	1617	68.5	16	26.6	0.922

As a consequence, the N−O bond distance is shorter in **3** in comparison to **4**, and the Rh−N bond distance is longer in **3** than in **4**.

The N−O bond length in complex **4** (1.184(4) Å) is longer than the N−O bond length (1.175(7) Å) in complex **2**, in agreement with the bent Rh−N−O angle in complex **4** (127.4(3)°) in comparison to the close-to-linear Rh−N−O angle in complex **2** (159.9(6)°). The IR spectra are in line with this structure; an absorption at 1618 cm^{-1} was observed for complex **4**, while in the case of complex **2** absorptions at higher frequencies were noted, 1841, 1817 cm^{-1} (slightly split).

In conclusion, addition of a chloride ligand to the linear nitrosyl complex **2** results in the transfer of electron density from the electron-rich Rh(I) center to the NO ligand, causing the MNO group to bend and forming the Rh(III) complex **4**. The driving force for the linear to bent geometry conversion is the population of an orbital that is π antibonding between the metal and the NO in the linear geometry but π bonding and thus more stable in the bent geometry. A relevant example of linear-to-bent NO conformation change was reported for the addition of a halide ion to the linear NO complex $[Co(das)_2(NO)]^{2+}$ (das: *o*-phenylenebis(dimethylarsine)), which produced the complex $[Co(das)_2(NO)X]^+$, containing a strongly bent MNO unit.[22] In this case the π-antibonding orbital is populated by the pair of electrons from the halide ligand.

IR Study of Solvent Interactions of the NO Ligand of Complex 2. Solvents can interact with the nitrosyl group via the metal center, and this is particularly evident in the case of the coordinatively unsaturated complex **2** (Table 4).

The two most common solvent parameters used to rationalize solvent-ν_{NO} trends are the Gutmann donor number (DN) and the Gutmann acceptor number (AN) of the solvent employed. These parameters may be used to rank organic solvents in order of their donor and acceptor abilities, respectively. Another empirical measure of solvent polarity is the *Z*-value, which is based on the position of the charge-transfer band of 1-ethyl-4-carbomethoxypyridinium iodide in a given solvent (Table 4).[23]

As shown in Figure 4, as the DN of the solvent used to record the IR spectra increases, a significant decrease in the ν_{NO} of complex **2** is observed; this is consistent with the increased back-donation of electron density from rhodium to the nitrosyl ligand due to the enhanced electron richness of the metal center.

In addition, $^{31}P\{^1H\}$ NMR shows the characteristic shift of bent NO complexes for complex **2** in CH_3CN, CH_3OH, and DMSO (Table 5).

For comparison, $^{31}P\{^1H\}$ NMR and $^1J_{RhP}$ data of the bent NO complexes **3**, **4**, and **6** are summarized in Table 6.

Thus, the large decrease in ν_{NO} as well as the $^{31}P\{^1H\}$ NMR shift strongly indicates that in CH_3CN, CH_3OH, and DMSO, complex **2** behaves as a bent nitrosyl complex. The following equilibrium is proposed for the solvents mentioned above (Scheme 4).

(22) Evans, W.; Zink, J. *J. Am. Chem. Soc.* **1981**, *103*, 2635–2640.
(23) Kosower, E. M. *J. Am. Chem. Soc.* **1958**, *80*, 3253–3260.

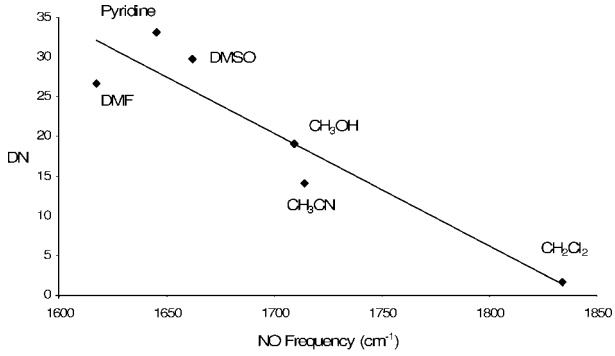

Figure 4. Gutmann donor number (DN) vs IR frequencies of the NO ligand in complex **2** in various solvents.

Table 5. IR Frequencies and $^{31}P\{^1H\}$ NMR of Complex 2 in Different Solvents

solvent	ν_{NO} (cm^{-1})	$^{31}P\{^1H\}$ NMR (ppm)	$^1J_{RhP}$ (Hz)
CH_2Cl_2	1834	104.02	130.6
CH_3CN	1714	83.12	138.7
CH_3OH	1709	98.56	143.3
DMSO	1662	83.08	140.9

Table 6. $^{31}P\{^1H\}$ NMR of Bent NO Complexes

complex	$^{31}P\{^1H\}$ NMR (ppm)	$^1J_{RhP}$ (Hz)
3 (CH_2Cl_2)	91.27	128.5
4 (C_6D_6)	74.93	143.9
6 (CH_2Cl_2)	73.98	105.1

Scheme 4[a]

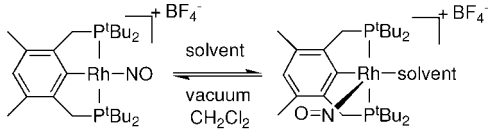

[a] Solvent: CH_3CN, CH_3OH, and DMSO.

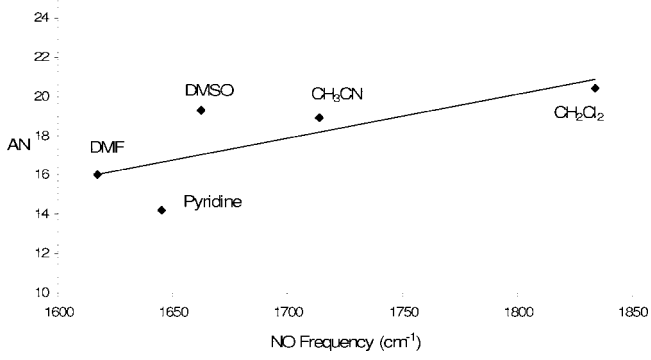

Figure 5. Gutmann acceptor number (AN) vs IR frequencies of the NO ligand in complex **2** in various solvents.

In contrast, as the AN of the solvent increases, ν_{NO} of complex **2** also increases (Figure 5), indicating strengthening of the NO bond, with the back-donation of electron density from rhodium to the π^* orbitals of the nitrosyl ligand being less favored.

As we can see, comparison of the ν_{NO} with *Z*-values obtained in solvents of different polarity can lead to interesting conclusions about NO bent or linear stabilization (Figure 6). In high *Z*-value (polar) solvents, lower ν_{NO} were observed, favoring bent nitrosyl complexes, while in low *Z*-value solvents, the obtained higher ν_{NO} suggests stabilization of linear nitrosyl complexes.

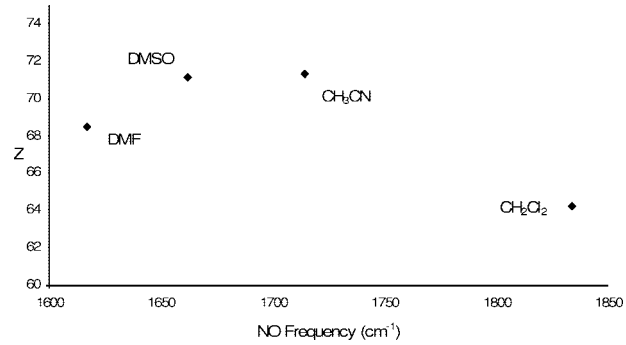

Figure 6. *Z*-values vs IR frequencies of the NO ligand in complex **2** in various solvents.

Scheme 5

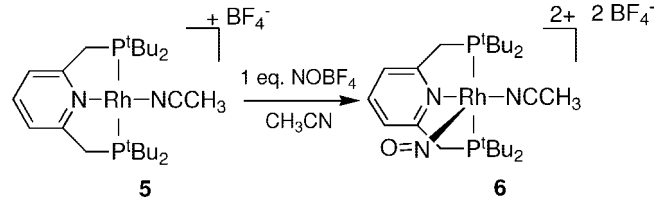

Reaction of Rh(PCP^{t}Bu)(NO)(Cl) (4) with $HBF_4 \cdot O(C_2H_5)_2$. Formation of Rh(PCP^{t}Bu)(NO)][BF_4] (2) and HCl. Addition of H^+ to the bent-NO complex **4** resulted only in chloride abstraction to form complex **2**, and no formation of a nitroxyl complex was observed (Scheme 3).

Synthesis of the PNP-Nitrosyl Rh(III) Complex (6). In order to study the effect of changing the PCP ligand to a PNP-type ligand on the mode of bonding of the nitrosyl ligand, the highly electron-donating PNP^{t}Bu (PNP^{t}Bu = 2,6-bis(di-*tert*-butylphosphinomethyl)pyridine)[10] pincer-type ligand was used. Upon reaction of the monocationic (PNP^{t}Bu)Rh(I),[10] complex **5**, with NO^+, the pentacoordinate complex **6** was obtained (Scheme 5).

In comparison with the formation of complex **2** by reaction of the dinitrogen complex **1** with $NOBF_4$ (Scheme 1), in this case there is no ligand substitution and NO^+ oxidizes the metal center from Rh(I) to Rh(III), becoming NO^-. The phosphines exhibit a doublet at δ 73.98 with a $^1J_{Rh,P}$ = 105.1 Hz. The CH_3CN molecule remains coordinated to the rhodium center, as confirmed by IR spectroscopy, which shows a weak band corresponding to the coordinated CN stretching mode vibration at 2335 cm^{-1}. A signal corresponding to the nitrosyl ligand was observed at 1703 cm^{-1} as a strong, sharp band, verified by its ^{15}N-labeled nitrosyl derivative with a frequency at 1671 cm^{-1}. In the ^1H NMR the acetonitrile protons appear at 2.98 ppm with a chemical shift significantly downfield from that of free acetonitrile, indicating less back-bonding from the metal to the acetonitrile ligand due to the presence of NO, a strong π-acceptor. A broad singlet at 829.76 ppm was observed in the ^{15}N NMR spectrum of the ^{15}N-enriched nitrosyl complex **6**, confirming the presence of a bent nitrosyl, as it is in the range of the bent nitrosyl complexes **3** and **4**. An X-ray diffraction study of crystals of **6**, grown by slow evaporation of an acetonitrile solution at room temperature, reveals the expected square-pyramidal geometry already observed for the pentacoordinated nitrosyl pincer-type rhodium complexes **3** and **4** (Figure 7).

The nitrosyl ligand is located at the apical position, and the acetonitrile molecule is *trans* to the *ipso* nitrogen. The Rh−N−O angle is 122.4(2)° and the N−O bond length is 1.151(4) Å (Table 7), both in the range of angles and bond lengths observed

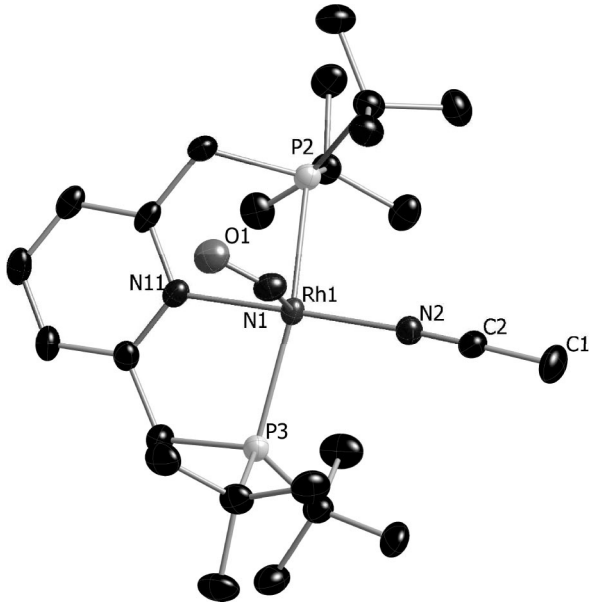

Figure 7. ORTEP plot of complex **6** at the 50% probability level. Hydrogen atoms and counteranions are omitted for clarity.

Table 7. Selected Bond Lengths (Å) and Angles (deg) for 6

Rh(1)−N(1)	1.957(3)	Rh(1)−P(3)	2.3703(9)
Rh(1)−N(2)	2.030(3)	N(1)−O(1)	1.151(4)
Rh(1)−N(11)	2.062(3)	N(2)−C(2)	1.137(4)
Rh(1)−P(2)	2.3524(9)	C(1)−C(2)	1.459(4)
Rh(1)−N(1)−O(1)	122.4(2)	C(1)−C(2)−N(2)	178.2(4)
N(1)−Rh(1)−N(2)	89.76(11)	N(2)−Rh(1)−P(2)	96.67(8)
N(1)−Rh(1)−P(2)	95.74(9)	N(2)−Rh(1)−P(3)	95.26(8)
N(1)−Rh(1)−P(3)	98.77(9)	P(2)−Rh(1)−P(3)	161.21(3)
N(1)−Rh(1)−N(11)	93.93(11)	P(2)−Rh(1)−N(11)	83.08(8)
N(2)−Rh(1)−N(11)	176.31(10)	P(3)−Rh(1)−N(11)	84.08(8)
Rh(1)−N(2)−C(2)	175.5(3)		

Scheme 6

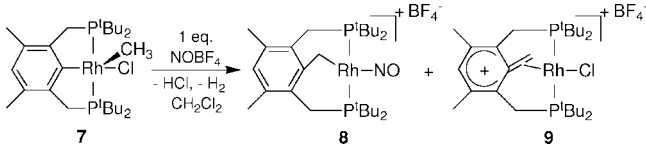

in the bent nitrosyl rhodium systems already described for complexes **3** and **4**. A similar PNP′Bu rhodium nitrosyl complex was recently reported.[16a]

Synthesis of an Unusual Linear Nitrosyl Rh(I) Phosphine Complex (8). Reaction of NO^+ with the known methyl chloride Rh(III) complex **7**[8] resulted in formation of the peculiar linear nitrosyl **8** (Scheme 6).

The mechanism of the nitrosyl-induced rearrangement of the Rh(III) precursor **7** probably involves initial electrophilic attack of NO^+ on the metal center, giving complex **A** (Scheme 7).

This unstable electron-poor species may form the methyl arenium complex **B** by methyl migration to the aromatic ring. Such a 1,2-methyl shift was already observed in the synthesis of σ-arenium complexes.[24] Complex **B** can then undergo β-hydrogen elimination, giving complex **C**, which after HCl elimination forms the cationic benzylic Rh(I) complex **8**. A similar neutral carbonyl benzylic Rh(I) complex was reported.[24] Due to the generation of HCl in situ, the known compound **9** is also obtained as a byproduct by reaction of complex **7** with

(24) Vigalok, A.; Rybtchinski, B.; Shimon, L. J. W.; Ben-David, Y.; Milstein, D. *Organometallics* **1999**, *18*, 895–905.

Scheme 7. Postulated Mechanism of Formation of Complex 8[a]

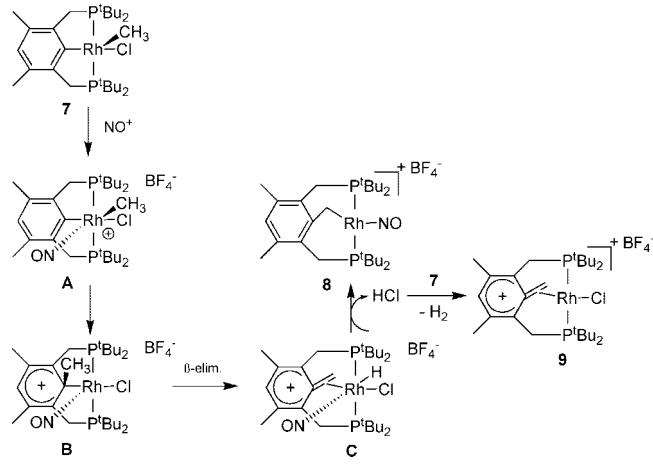

[a] The spectroscopically characterized compounds are numbered; postulated intermediates are assigned with capital letters.

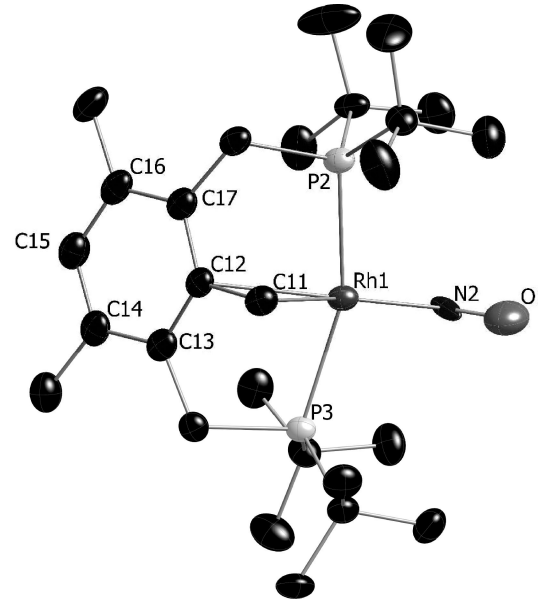

Figure 8. ORTEP plot of complex **8** at the 50% probability level. Hydrogen atoms and counteranion are omitted for clarity.

HCl.[24] Complex **8** exhibits in the $^{31}P\{^1H\}$ NMR a doublet at δ 109.62 with a $^1J_{Rh,P} = 153.7$ Hz. It also shows in the ^1H NMR spectrum a triplet of doublets at 3.46 ppm ($^2J_{Rh,H} = 2.9$ Hz) due to the metal-bound benzylic group. ^{15}N NMR spectroscopy of the ^{15}N-enriched nitrosyl complex **8** gives rise to a doublet at δ 377.06 ppm with a $^1J_{Rh,N}$ of 33.6 Hz, characteristic of a bound linear nitrosyl ligand.[19] The IR spectrum obtained in the solid state shows a signal characteristic of a nitrosyl ligand at 1698 cm^{-1} (^{15}N-labeled complex **8**: 1666 cm^{-1}).

A single-crystal X-ray analysis of **8** (Figure 8) confirmed that it is a Rh(I) complex with the rhodium atom situated in the center of a square-planar geometry and a close-to-linear nitrosyl group *trans* to the methylene carbon, with a Rh−N−O angle of 156.3(5) Å (Table 8), in the range of the observed Rh−N−O angles for complex **2** (159.9(6)°).

The coordinated methylene is tilted out of the plane, with a Rh(1)−C(11)−C(12) angle of 87.9(2)°. The observed N−O bond length of 1.049(5) Å is particularly shorter in comparison to the N−O bond distance of 1.176(7) Å in the linear nitrosyl complex **2**, although the ν(NO) stretching vibration is more than

Table 8. Selected Bond Lengths (Å) and Angles (deg) for 8

Rh(1)−C(11)	2.078(4)	C(12)−C(13)	1.409(6)
Rh(1)−C(12)	2.509(4)	C(13)−C(14)	1.408(6)
C(11)−C(12)	1.485(6)	C(14)−C(15)	1.383(6)
Rh(1)−N(2)	1.832(4)	C(15)−C(16)	1.394(6)
N(2)−O(1)	1.049(5)	C(16)−C(17)	1.406(6)
Rh(1)−P(2)	2.3790(10)	C(17)−C(12)	1.404(6)
Rh(1)−P(3)	2.3813(10)		
Rh(1)−N(2)−O(1)	156.3(5)	Rh(1)−C(11)−C(12)	87.9(2)
N(2)−Rh(1)−P(2)	99.17(11)	C(11)−C(12)−Rh(1)	55.86(19)
N(2)−Rh(1)−P(3)	99.03(10)	C(13)−C(12)−C(17)	122.5(4)
N(2)−Rh(1)−C(11)	146.5(2)	C(14)−C(15)−C(16)	124.7(4)
P(2)−Rh(1)−P(3)	160.98(4)	C(12)−C(13)−C(14)	118.1(4)
C(11)−Rh(1)−C(12)	36.27(14)	C(13)−C(14)−C(15)	117.9(4)

100 cm^{-1} lower for **8** as compared to **2** (Table 9). This unusual result found for **8** suggests probably that N−O and Rh−N−O bending modes could be highly mixed[25] or that other experimental effects such as thermal motion or positional disorder of the nitrosyl atoms could be present.[26] As mentioned for complex **2**, deviation from linearity of the nitrosyl ligand in complex **8** is probably a result of strong σ-donation of the aryl ring.[21]

Distinguishing between Geometries of Nitrosyl Complexes Based on ^{15}N NMR. Table 9 shows ^{15}N NMR measurements for linear and bent nitrosyl ligands of rhodium complexes with pincer-type ligands and NO stretching frequencies for comparison.

While IR data are not very indicative, there are two well-defined groups in the ^{15}N NMR measurements of the above complexes, demonstrating that ^{15}N NMR spectroscopy is particularly suitable for distinguishing between bent and linear M−N−O conformations because of the large downfield shift (by hundreds of ppm) observed for the bent as compared with the linear nitrosyl ligands (ca. 377 ppm for the linear nitrosyl complexes **2** and **8**, as compared with ca. 830−840 ppm for the bent nitrosyl complexes **3**, **4**, and **6**). Similar observations were reported for other linear and bent rhodium nitrosyl complexes.[19]

For ^{15}N-labeled nitrosyl rhodium complexes also the coupling constant $J(^{103}Rh,^{15}N)$ can be measured, which may be expected to show a large dependence on the hybridization of the nitrosyl nitrogen atom. For the complexes presented in this work, in the case of linear NO complexes **2** and **8**, with sp-hybridized nitrogen, a doublet is observed with $J(^{103}Rh,^{15}N)$ ca. 35 Hz, whereas for the bent NO complexes **3**, **4**, and **6** in which the nitrogen atom is sp^2 hybridized, the $^{103}Rh-^{15}N$ coupling is not observed. These results are in accord with those reported by Bell et al., where a $J(^{103}Rh,^{15}N)$ of 52 Hz was found for a square-planar four-coordinated $\{RhNO\}^8$ linear nitrosyl complex, whereas square-pyramidal $\{RhNO\}^8$ bent nitrosyl complexes presented no coupling constant except for one example with a small $J(^{103}Rh,^{15}N)$ of 4.6 Hz, in agreement with the general observation that coupling constants to nitrogen carrying a lone pair may be small.[19]

Figure 9 shows that there is a tendency for the nitrogen shielding to decrease (the shift to low field increases) with increase of the Rh−N bond length. This bond length reflects the back-bonding in the MNO unit, which is very strong for the bent nitrosyl complexes **3**, **4**, and **6**; consequently the Rh−N bond distance is longer in comparison with linear nitrosyl complexes **2** and **8**, where back-donation is less strong. Thus, stronger deshielding is observed in the highly bent $\{RhNO\}^8$ nitrosyl complexes **3**, **4**, and **6** in comparison to the close-to-linear nitrosyl complexes **2** and **8**.

Summary

Linear nitrosyls of the cationic PCP^{t}Bu Rh(I) complexes **2** and **8** were prepared by electrophilic attack of NO^+ on the metal center of the Rh(I) dinitrogen complex **1** and on the methyl chloride Rh(III) complex **7**, respectively. Complex **2** exhibits interesting reactivity with CO, establishing an equilibrium in solution and in the solid state with the pentacoordinate CO adduct, the bent nitrosyl Rh(III) complex **3**. Nucleophilic attack of Cl^- on the metal center of complex **2** resulted in the selective formation of the bent nitrosyl complex **4**. Thus, the addition of a neutral or anionic nucleophile, CO and Cl^-, respectively, to complex **2** can induce a linear to bent NO conformation, with concomitant formal change in the metal oxidation states, from Rh^I to Rh^{III}.

The IR study of solvent interactions of the nitrosyl ligand in complex **2** in various solvents shows a correlation of the NO stretching frequency dependence with the DN, AN, and *Z* values of the solvents. The greater the DN or *Z*-value of the solvent, the lower the ν_{NO} observed, whereas as the AN of the solvent increases, ν_{NO} of complex **2** also increases. Consequently, comparison of the ν_{NO} obtained in solvents of different polarity with these solvent parameters can lead to useful conclusions about NO conformation. Moreover, the spectacular IR frequency shift strongly indicates that solvents such as CH_3CN, CH_3OH, and DMSO are also able to establish a linear-to-bent nitrosyl equilibrium such as the one described for CO.

Complex **2** was also prepared by chloride abstraction of complex **4** with $HBF_4 \cdot O(C_2H_5)_2$. As expected, treatment of complex **2** with electrophiles such as CH_3I resulted in no reaction, as a result of low electron density at the metal center. Also, no reaction was observed when complex **2** was treated with H_2. In the case of the reaction of NO^+ with (PNP^{t}Bu)Rh(CH_3CN) **5**, CH_3CN did not dissociate and the bent nitrosyl (PNP^{t}Bu)Rh(III)(NO)(CH_3CN) complex **6** was formed. Although IR generally provides indirect information about the structure of nitrosyl complexes, both in solution and in the solid state, there is an overlap in the 1600−1720 cm^{-1} region, which comprises N−O stretching frequencies for both linear and bent nitrosyl ligands, limiting the usefulness of this technique as a structural probe.[27] Complexes **6** and **8** are examples of such an overlap. On the other hand, ^{15}N NMR spectroscopy of ^{15}N-enriched nitrosyl complexes has shown that the NO nitrogen atom is deshielded by hundreds of ppm in bent as compared with linear nitrosyl ligands. ^{15}N NMR spectroscopy is thus a useful probe for establishing the geometry and electronic distribution of nitrosyl ligands and of complexes in solution. In addition, X-ray structures of all nitrosyl complexes reported here confirmed the geometry suggested in solution by ^{15}N NMR spectroscopy. In the case of the tetracoordinate species the observed geometry is square-planar with a linear nitrosyl ligand occupying the position *trans* to the aromatic ring, with a Rh(I) metal center, and for the pentacoordinate complexes the geometry is square-pyramidal with a strongly bent apical nitrosyl, with a Rh(III) metal center. These results are in agreement with other $\{MNO\}^8$ square-planar and square-pyramidal complexes previously characterized.[3b]

Experimental Section

General Procedures. All experiments with metal complexes and phosphine ligands were carried out under an atmosphere of purified

(25) Immoos, C. E.; Sulc, F.; Farmer, P. J.; Czarnecki, K.; Bocian, D. F.; Levina, A.; Aitken, J. B.; Armstrong, R. S.; Lay, P. A. *J. Am. Chem. Soc.* **2005**, *127*, 814–815.

(26) Wyllie, G. R. A.; Scheidt, W. R. *Chem. Rev.* **2002**, *102*, 1067–1089.

(27) Haymore, B. L.; Ibers, J. A. *Inorg. Chem.* **1975**, *14*, 3060–3070.

Table 9. ^{15}N NMR and IR Measurements

complex	$\delta(^{15}N)^a$ (ppm)	$\nu(^{14}NO)$ (cm^{-1})^b	$\nu(^{15}NO)$ (cm^{-1})
[Rh(PCP^{t}Bu)(^{15}NO)]$^+$ (**2**-^{15}N)	377.88 (d, $^1J_{Rh,N}$ = 35.5 Hz)	1841:1817 (1:1)^c	1802:1777 (1:1)^c
[Rh(PCP^{t}Bu)(^{15}NO)(CO)]$^+$ (**3**-^{15}N)	837.14 (br s)	1686	1653
Rh(PCP^{t}Bu)(^{15}NO)(Cl) (**4**-^{15}N)	841.18 (br s)	1618	1585
[C$_5$H$_3$N(CH$_2$P(tBu)$_2$)$_2$Rh(CH$_3$CN)(^{15}NO)]$^{2+}$ (**6**-^{15}N)	829.76 (br s)	1703	1671
[Rh(PCP^{t}BuCH$_2$)(^{15}NO)]$^+$ (**8**-^{15}N)	377.06 (d, $^1J_{Rh,N}$ = 33.6 Hz)	1698	1666

^{a} In ppm relative to liquid ammonia; measured at −60 °C. ^{b} Solid, Nujol mull. ^{c} The splitting of the NO signal is a solid state effect, as it is not observed in solution (see Table 4). See ref 20.

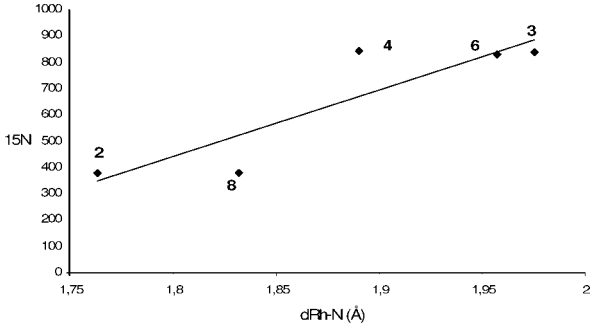

Figure 9. Correlation of the ^{15}N shift (ppm) vs Rh−N bond length (Å) for the nitrosyl complexes **2**, **3**, **4**, **6**, and **8**.

nitrogen in a Vacuum Atmospheres glovebox equipped with a MO 40-2 inert gas purifier or using standard Schlenk techniques. All solvents were reagent grade or better. All nondeuterated solvents were refluxed over sodium/benzophenone ketyl and distilled under an argon atmosphere. Deuterated solvents were dried over 4 Å molecular sieves. Commercially available reagents were used as received. [Rh(COE)$_2$Cl]$_2$,[28] Rh(PCP^{t}Bu)(CH$_3$)Cl,[8] Rh(PCP^{t}Bu)N$_2$,[18] [Rh(PNP^{t}Bu)(CH$_3$CN)]BF$_4$,[10] 1,3-bis[(di-*tert*-butylphosphino)methyl]-2,4,6-trimethylbenzene (PCP^{t}Bu),[8] 2,6-bis(di-*tert*-butylphosphinomethyl)pyridine (PNP^{t}Bu),[10] and ^{15}NOBF$_4$[29] were prepared according to literature procedures.

^{1}H, ^{13}C, ^{15}N, ^{19}F, and ^{31}P NMR spectra were recorded using a Bruker DPX-250, a Bruker AMX-400, and an Avance 500 NMR spectrometer. All spectra were recorded at 23 °C unless otherwise noted. ^{1}H and ^{13}C{^{1}H} NMR chemical shifts are reported in ppm downfield from tetramethylsilane. ^{1}H NMR chemical shifts were referenced to the residual hydrogen signal of the deuterated solvent (7.24 ppm, choloform; 7.15 ppm, benzene; 5.32 ppm, dichloromethane; 1.96 ppm, acetonitrile). In ^{13}C{^{1}H} NMR measurements the signals of deuterated chloroform (77.0 ppm), deuterated benzene (128.0 ppm), deuterated dichloromethane (53.8 ppm), and deuterated acetonitrile (1.3 ppm) were used as a reference. ^{31}P NMR chemical shifts are reported in ppm downfield from H_3PO_4 and referenced to an external 85% solution of phosphoric acid in D_2O. ^{15}N NMR chemical shifts are reported in ppm relative to liquid ammonia. Abbreviations used in the description of NMR data are as follows: br, broad; s, singlet; d, doublet; t, triplet; q, quartet; m, multiplet; v, virtual; dist, distorted. Elemental analyses were performed by H. Kolbe, Mikroanalytisches Laboratorium, Mülheim, Germany.

Reaction of Rh(PCP^{t}Bu)N$_2$ (1) with NOBF$_4$. Formation of [Rh(PCP^{t}Bu)(NO)][BF$_4$] (2). A cold orange-brown solution of **1** (20 mg, 0.036 mmol) in dioxane (1 mL) was added to cold solid NOBF$_4$ (4.2 mg, 0.036 mmol), resulting in the formation of a dark green precipitate. The suspension was stirred at room temperature for 4 h. The green precipitate was filtered and washed with ether and dioxane, giving 15 mg of **2** in 66% yield. Single crystals suitable for X-ray diffraction were obtained by slow diffusion of pentane into a concentrated solution of **2** in CH_2Cl_2 at room temperature.

Characterization of 2. ^{31}P{^{1}H} NMR (CD_2Cl_2): 104.02 (d, $^1J_{RhP}$ = 130.6 Hz). ^{1}H NMR (CD_2Cl_2): 6.76 (s, 1H, Rh-***Ar***), 3.70 (vt, J_{PH} = 4.4 Hz, 4H, 2 Ar-C***H***$_2$-P), 2.26 (s, 6H, 2 Ar-C***H***$_3$), 1.48 (vt, J_{PH} = 7.4 Hz, 36H, 4 (C***H***$_3$)$_3$C-P). ^{13}C{^{1}H} NMR (CD_2Cl_2): 170.60 (dt, $^1J_{RhC}$ = 36.5 Hz, $^2J_{PC}$ = 2.5 Hz, C$_{ipso}$, Rh-***Ar***), 154.28 (vtd, J_{PC} = 10.3 Hz, J_{RhC} = 4.2 Hz, Rh-***Ar***), 133.86 (s, C$_{para}$, Rh-***Ar***), 133.13 (vt, J_{PC} = 9.3 Hz, Rh-***Ar***), 38.40 (vt, J_{PC} = 8.5 Hz, (CH$_3$)$_3$***C***-P), 32.73 (vtd, J_{PC} = 13.6 Hz, $^2J_{RhC}$ = 2.5 Hz, Ar-***C***H$_2$-P), 29.75 (vt, J_{PC} = 2.3 Hz, (***C***H$_3$)$_3$C-P), 22.54 (s, ***C***H$_3$−Ar) (assignment of ^{13}C{^{1}H} NMR signals was confirmed by ^{13}C DEPT135). IR ν (mineral oil; cm^{-1}): 1841, 1817 (s, slightly split, NO). IR ν (CH_2Cl_2; cm^{-1}): 1834 (s, NO). Anal. Calcd: C, 48.69; H, 7.39. Found: C, 48.76; H, 7.34.

X-ray Structural Analysis of 2. ***Crystal data*****:** $C_{26}H_{47}NOP_2Rh + BF_4$, orange/blue, plate, 0.1 × 0.1 × 0.05 mm^3, triclinic; *P*1(#1); a = 8.028(2) Å, b = 8.489(2) Å, c = 11.453(2) Å; α = 79.77(3)°, β = 78.72(3)°, γ = 83.25(3)°, from 20 degrees of data; T = 120(2) K; V = 750.5(3) Å^3, Z = 1; fw = 641.31; D_c = 1.419 Mg/m^3; μ = 0.720 mm^{-1}. *Data Collection and Processing:* Nonius KappaCCD diffractometer, Mo Kα (λ = 0.71073 Å), graphite monochromator; $0 \le h \le 10$, $-10 \le k \le 10$, $-14 \le l \le 14$, frame scan width = 2.0°, scan speed 1.0° per 30 s, typical peak mosaicity 0.67°, 13 101 reflections collected, 3370 independent reflections (R_{int} = 0.061). The data were processed with Denzo-Scalepack. *Solution and Refinement:* The structure was solved by direct methods with SHELXS-97. Full-matrix least-squares refinement based on F^2 with SHELXL-97; 340 parameters with 3 restraints, final R_1 = 0.0369 (based on F^2) for data with $I > 2\sigma(I)$ and R_1 = 0.0394 on 3368 reflections, goodness-of-fit on F^2 = 1.063, largest electron density peak = 0.529 e Å^{-3}.

Characterization of ^{15}N-Labeled 2. ^{15}N NMR (CD_2Cl_2, at −60 °C): 377.88 (d, $^1J_{RhN}$ = 35.5 Hz). ^{31}P{^{1}H} NMR (CD_2Cl_2): 104.18 (d, $^1J_{RhP}$ = 129.6 Hz). ^{1}H NMR (CD_2Cl_2): 6.70 (s, 1H, Rh-***Ar***), 3.60 (vt, J_{PH} = 4.3 Hz, 4H, 2 Ar-C***H***$_2$-P), 2.18 (s, 6H, 2 Ar-C***H***$_3$), 1.39 (vt, J_{PH} = 7.3 Hz, 36H, 4 (C***H***$_3$)$_3$C-P). ^{13}C{^{1}H} NMR (CD_2Cl_2): 170.54 (dd, $^1J_{RhC}$ = 35.3 Hz, $^2J_{NC}$ = 15.8 Hz, C$_{ipso}$, Rh-***Ar***), 154.14 (vt, J_{PC} = 10.2 Hz, Rh-***Ar***), 133.83 (s, C$_{para}$, Rh-***Ar***), 133.16 (vt, J_{PC} = 9.4 Hz, Rh-***Ar***), 38.40 (vt, J_{PC} = 8.4 Hz, (CH$_3$)$_3$***C***-P), 32.71 (vtd, J_{PC} = 13.7 Hz, $^2J_{RhC}$ = 2.3 Hz, Ar-***C***H$_2$-P), 29.79 (vt, J_{PC} = 2.0 Hz, (***C***H$_3$)$_3$C-P), 22.60 (s, ***C***H$_3$-Ar) (assignment of ^{13}C{^{1}H} NMR signals was confirmed by ^{13}C DEPT135). IR ν (mineral oil; cm^{-1}): 1802, 1777 (s, slightly split, ^{15}NO).

Reaction of [Rh(PCP^{t}Bu)(NO)][BF$_4$] (2) with CO$_{(g)}$ in CD$_2$Cl$_2$ and in the Solid State. Formation of [Rh(PCP^{t}Bu)(NO)(CO)][BF$_4$] (3). Upon bubbling carbon monoxide through a solution of **2** in CD_2Cl_2, an immediate color change from green to brown took place, and quantitative formation of the pentacoordinate CO adduct **3** was observed by ^{31}P{^{1}H} NMR. Complex **3** is stable in solution at low temperature, but at room temperature it is stable only under excess CO. The reaction appeared to be reversible, with complex **2** being recovered from a methylene chloride solution of **3** upon standing at room temperature or upon evaporation of the methylene chloride solution under vacuum. Single crystals suitable for X-ray diffraction were obtained from a concentrated solution of **3** in CH_2Cl_2 at −30 °C.

(28) Herde, J. L.; Senoff, C. V. *Inorg. Nucl. Chem. Lett.* **1971**, *7*, 1029–1031.

(29) Connelly, N. G.; Draggett, P. T.; Green, M.; Kuc, T. A. *J. Chem. Soc. Dalton Trans.* **1977**, 70–73.

Similarly, when carbon monoxide was added to **2** in the solid state, a color change from green to brown took place slowly, with quantitative formation of the pentacoordinate CO adduct **3**. Again, complex **2** was recovered upon vacuum drying of **3** during several days.

Characterization of 3 ($T = -30$ °C). $^{31}P\{^1H\}$ NMR (CD_2Cl_2): 91.27 (d, $^1J_{RhP} = 128.5$ Hz). ^1H NMR (CD_2Cl_2): 6.92 (s, 1H, Rh-***Ar***), 3.51 (AB quartet, $^2J_{HH} = 17.6$ Hz, 4H, 2 Ar-C***H***$_2$-P), 2.37 (s, 6H, 2 Ar-C***H***$_3$), 1.16 (vt, $J_{PH} = 6.9$ Hz, 18H, 2 (C***H***$_3$)$_3$C-P), 1.15 (vt, $J_{PH} = 6.9$ Hz, 18H, 2 (C***H***$_3$)$_3$C-P). $^{13}C\{^1H\}$ NMR (CD_2Cl_2): 189.55 (dt, $^1J_{RhC} = 47.3$ Hz, $^2J_{PC} = 9.7$ Hz, Rh-***C***O), 168.93 (d, $^1J_{RhC} = 32.0$ Hz, C_{ipso}, Rh-***Ar***), 145.91 (vt, $J_{PC} = 7.6$ Hz, Rh-***Ar***), 133.35 (vt, $J_{PC} = 9.1$ Hz, Rh-***Ar***), 131.0 (s, C_{para}, Rh-***Ar***), 37.24 (vt, $J_{PC} = 8.6$ Hz, (CH$_3$)$_3$***C***-P), 36.86 (vt, $J_{PC} = 8.5$ Hz, (CH$_3$)$_3$***C***-P), 32.28 (vt, $J_{PC} = 12.3$ Hz, Ar-***C***H$_2$-P), 30.07 (s, (***C***H$_3$)$_3$C-P), 28.09 (s, (***C***H$_3$)$_3$C-P), 22.55 (s, ***C***H$_3$-Ar) (assignment of $^{13}C\{H\}$ NMR signals was confirmed by ^{13}C DEPT135). IR ν (CH_2Cl_2; cm^{-1}): 2080, 2065 (s, CO, slightly split in methylene chloride), 1699 (s, NO). IR ν (mineral oil; cm^{-1}): 2087, 2071 (s, slightly split, CO), 1686 (s, NO). Anal. Calcd: C, 48.45; H, 7.08; N, 2.09. Found: C, 48.22; H, 6.95; N, 2.12.

X-ray Structural Analysis of 3. ***Crystal data:*** $C_{27}H_{47}NO_2P_2Rh + BF_4$, yellow-orange, prism, $0.05 \times 0.02 \times 0.02$ mm^3, monoclinic; *P*2(1); $a = 8.2140(2)$ Å, $b = 22.253(5)$ Å, $c = 8.3550(2)$ Å; $\beta = 93.05(3)°$, from 18 degrees of data; $T = 120(2)$ K; $V = 1525.0(6)$ Å^3, $Z = 2$; fw = 669.32; $D_c = 1.458$ Mg/m^3; $\mu = 0.714$ mm^{-1}. *Data Collection and Processing:* Nonius KappaCCD diffractometer, Mo Kα ($\lambda = 0.71073$ Å), graphite monochromator; $-10 \le h \le 10$, $0 \le k \le 27$, $0 \le l \le 10$, frame scan width = 1.0°, scan speed 1.0° per 200 s, typical peak mosaicity 0.73°, 20 071 reflections collected, 3154 independent reflections ($R_{int} = 0.110$). The data were processed with Denzo-Scalepack. *Solution and Refinement:* The structure was solved by direct methods with SHELXS-97. Full-matrix least-squares refinement based on F^2 with SHELXL-97; 342 parameters with 1 restraint, final $R_1 = 0.0514$ (based on F^2) for data with $I > 2\sigma(I)$, $R_1 = 0.0608$ on 3138 reflections, goodness-of-fit on $F^2 = 1.092$, largest electron density peak = 0.897 e Å^{-3}.

Characterization of ^{15}N-Labeled 3. ^{15}N NMR (CD_2Cl_2, at −60 °C): 837.14 (br s). $^{31}P\{^1H\}$ NMR (CD_2Cl_2, at −30 °C): 91.45 (d, $^1J_{RhP} = 127.9$ Hz). ^1H NMR (CD_2Cl_2, at −30 °C): 6.92 (s, 1H, Rh-***Ar***), 3.51 (AB quartet, $^2J_{HH} = 17.8$ Hz, 4H, 2 Ar-C***H***$_2$-P), 2.37 (s, 6H, 2 Ar-C***H***$_3$), 1.14 (vt, $J_{PH} = 6.7$ Hz, 18H, 2 (C***H***$_3$)$_3$C-P), 1.16 (vt, $J_{PH} = 6.7$ Hz, 18H, 2 (C***H***$_3$)$_3$C-P). $^{13}C\{^1H\}$ NMR (CD_2Cl_2, at −30 °C): 189.55 (dt, $^1J_{RhC} = 47.3$ Hz, $^2J_{PC} = 9.8$ Hz, Rh-***C***O), 168.95 (d, $^1J_{RhC} = 32.0$ Hz, C_{ipso}, Rh-***Ar***), 145.91 (vt, $J_{PC} = 7.5$ Hz, Rh-***Ar***), 133.36 (vt, $J_{PC} = 9.1$ Hz, Rh-***Ar***), 131.0 (s, C_{para}, Rh-***Ar***), 37.24 (vt, $J_{PC} = 8.7$ Hz, (CH$_3$)$_3$***C***-P), 36.87 (vt, $J_{PC} = 8.5$ Hz, (CH$_3$)$_3$***C***-P), 32.29 (vt, $J_{PC} = 12.3$ Hz, Ar-***C***H$_2$-P), 30.08 (s, (***C***H$_3$)$_3$C-P), 28.09 (s, (***C***H$_3$)$_3$C-P), 22.57 (s, ***C***H$_3$-Ar) (assignment of $^{13}C\{H\}$ NMR signals was confirmed by ^{13}C DEPT135). IR ν (mineral oil; cm^{-1}): 2087, 2071 (s, slightly split, CO), 1653 (s, ^{15}NO).

Reaction of [Rh(PCP^{t}Bu)(NO)][BF$_4$] (2) with LiCl. Formation of Rh(PCP^{t}Bu)(NO)(Cl) (4). Benzene was added to a mixture of solid **2** (20 mg, 0.031 mmol) and solid LiCl (in excess). The suspension was stirred at room temperature for 30 min, resulting in a color change from green to brown. $^{31}P\{^1H\}$ NMR revealed quantitative formation of **4** as a single product. The suspension was filtered, the solvent was evaporated, and the remaining solid was extracted with pentane. Evaporation of pentane under vacuum gave 17 mg of **4** in 94% yield. Single crystals suitable for X-ray diffraction were obtained by crystallization from a concentrated solution of **4** in ether at −30 °C.

Characterization of 4. $^{31}P\{^1H\}$ NMR (C_6D_6): 74.93 (d, $^1J_{RhP} = 143.9$ Hz). ^1H NMR (C_6D_6): 6.66 (s, 1H, Rh-***Ar***), 3.08 (AB quartet, $^2J_{HH} = 17.1$ Hz, 4H, Ar-C***H***$_2$-P), 2.19 (s, 6H, 2 Ar-C***H***$_3$), 1.21 (vt, $J_{PH} = 6.4$ Hz, 18H, 2 (C***H***$_3$)$_3$C-P), 1.15 (vt, $J_{PH} = 6.9$ Hz, 18H, 2 (C***H***$_3$)$_3$C-P). $^{13}C\{^1H\}$ NMR (C_6D_6): 167.0 (d, $^2J_{RhC} = 39.0$ Hz, C_{ipso}, Rh-***Ar***), 145.11 (vtd, $J_{PC} = 8.4$ Hz, $J_{RhC} = 1.5$ Hz, Rh-***Ar***), 130.92 (vt, $J_{PC} = 8.4$ Hz, Rh-***Ar***), 128.30 (s, C_{para},Rh-***Ar***), 36.71 (vtd, $J_{PC} = 6.9$ Hz, $^2J_{RhC} = 0.8$ Hz, (CH$_3$)$_3$***C***-P), 35.38 (vtd, $J_{PC} = 6.9$ Hz, $^2J_{RhC} = 0.8$ Hz, (CH$_3$)$_3$***C***-P), 30.47 (vtd, $J_{PC} = 10.4$ Hz, $^2J_{RhC} = 2.3$ Hz, Ar-***C***H$_2$-P), 30.24 (vt, $J_{PC} = 2.3$ Hz, (***C***H$_3$)$_3$C-P), 28.64 (vt, $J_{PC} = 2.3$ Hz, (***C***H$_3$)$_3$C-P), 22.43 (s, ***C***H$_3$-Ar) (assignment of $^{13}C\{H\}$ NMR signals was confirmed by ^{13}C DEPT135). IR ν (mineral oil; cm^{-1}): 1618 (s, NO). IR ν (C_6H_6; cm^{-1}): 1625 (s, NO). Anal. Calcd: C, 52.93; H, 8.04. Found: C, 52.76; H, 7.93.

X-ray Structural Analysis of 4. ***Crystal data:*** $C_{26}H_{47}NOP_2ClRh$, orange, needles, $0.2 \times 0.05 \times 0.05$ mm^3, monoclinic; *P*2(1)/*n* (#14); $a = 8.6274(2)$ Å, $b = 23.1733(7)$ Å, $c = 14.4164(4)$ Å; $\beta = 94.4112(18)°$, from 20 degrees of data; $T = 120(2)$ K; $V = 2873.67(14)$ Å^3, $Z = 4$; fw = 589.95; $D_c = 1.364$ Mg/m^3; $\mu = 0.817$ mm^{-1}. *Data Collection and Processing:* Nonius KappaCCD diffractometer, Mo Kα ($\lambda = 0.71073$ Å), graphite monochromator; $-10 \le h \le 10$, $-27 \le k \le 27$, $-16 \le l \le 16$, frame scan width = 1.0°, scan speed 1.0° per 60 s, typical peak mosaicity 0.47°, 30 179 reflections collected, 4877 independent reflections ($R_{int} = 0.044$). The data were processed with Denzo-Scalepack. *Solution and Refinement:* The structure was solved by direct methods with SHELXS-97. Full-matrix least-squares refinement based on F^2 with SHELXL-97; 303 parameters with 0 restraints, final $R_1 = 0.0392$ (based on F^2) for data with $I > 2\sigma(I)$ and $R_1 = 0.0655$ on 4877 reflections, goodness-of-fit on $F^2 = 0.999$, largest electron density peak = 0.939 e Å^{-3}.

Characterization of ^{15}N-Labeled 4. ^{15}N NMR (CD_2Cl_2, at −60 °C): 841.18 (br s). $^{31}P\{^1H\}$ NMR (C_6D_6): 75.35 (d, $^1J_{RhP} = 143.5$ Hz). ^1H NMR (C_6D_6): 6.65 (s, 1H, Rh-***Ar***), 3.09 (AB quartet, $^2J_{HH} = 17.1$ Hz, 4H, Ar-C***H***$_2$-P), 2.18 (s, 6H, 2 Ar-C***H***$_3$), 1.21 (vt, $J_{PH} = 6.4$ Hz, 18H, 2 (C***H***$_3$)$_3$C-P), 1.15 (vt, $J_{PH} = 6.9$ Hz, 18H, 2 (C***H***$_3$)$_3$C-P). $^{13}C\{^1H\}$ NMR (C_6D_6): 166.1 (d, $^2J_{RhC} = 40.2$ Hz, C_{ipso}, Rh-***Ar***), 145.23 (vt, $J_{PC} = 8.1$ Hz, Rh-***Ar***), 131.44 (vt, $J_{PC} = 8.4$ Hz, $J_{RhC} = 1.4$ Hz, Rh-***Ar***), 128.12 (s, C_{para},Rh-***Ar***), 36.93 (br s, (CH$_3$)$_3$***C***-P), 35.84 (br s, (CH$_3$)$_3$***C***-P), 30.32 (vtd, $J_{PC} = 10.7$ Hz, $^2J_{RhC} = 2.4$ Hz, Ar-***C***H$_2$-P), 30.24 (vt, $J_{PC} = 2.3$ Hz, (***C***H$_3$)$_3$C-P), 28.80 (br s, (***C***H$_3$)$_3$C-P), 22.40 (s, ***C***H$_3$-Ar) (assignment of $^{13}C\{H\}$ NMR signals was confirmed by ^{13}C DEPT135). IR ν (mineral oil; cm^{-1}): 1585 (s, ^{15}NO).

Reaction of Rh(PCP^{t}Bu)(NO)(Cl) (4) with HBF$_4$·O(C$_2$H$_5$)$_2$. Formation of Rh(PCP^{t}Bu)(NO)][BF$_4$] (2) and HCl. To a brown solution of complex **4** (20 mg, 0.034 mmol) in benzene (1 mL) was added 1 equiv of HBF$_4$·O(C$_2$H$_5$)$_2$ (5 μL, 0.034 mmol), forming a dark green precipitate. The suspension was stirred at room temperature for 1 h. The green precipitate was filtered and washed with ether and dioxane, giving 21 mg of **2** in 97% yield.

Reaction of [C$_5$H$_3$N(CH$_2$P(^{t}Bu)$_2$)$_2$Rh(CH$_3$CN)]BF$_4$ (5) with NOBF$_4$. Formation of [C$_5$H$_3$N(CH$_2$P(^{t}Bu)$_2$)$_2$Rh(CH$_3$CN)(NO)][BF$_4$]$_2$ (6). A cold orange solution of **5** (20 mg, 0.032 mmol) in acetonitrile (1 mL) was added to cold solid $NOBF_4$ (3.7 mg, 0.032 mmol). The resulting solution was dark green colored. The mixture was stirred at room temperature for 12 h. Product **6** was further purified by crystallization from an acetonitrile solution at room temperature, resulting in 72% (17 mg) yield. Single crystals suitable for X-ray diffraction were obtained by crystallization from acetonitrile at room temperature.

Characterization of 6. $^{31}P\{^1H\}$ NMR (CD_2Cl_2): 73.98 (d, $^1J_{RhP} = 105.1$ Hz). ^1H NMR (CD_2Cl_2): 8.10 (t, $^3J_{HH} = 7.8$ Hz, 1H, pyridine-***H***4), 7.95 (d, $^3J_{HH} = 7.8$ Hz, 2H, pyridine-***H***3,5), 4.0 (AB quartet, $^2J_{HH} = 18.6$ Hz, 4H, Ar-C***H***$_2$-P), 2.98 (s, 3H, C***H***$_3$CN), 1.37 (vt, $J_{PH} = 7.7$ Hz, 18H, 2 (C***H***$_3$)$_3$C-P), 1.27 (vt, $J_{PH} = 8.0$ Hz, 18H, 2 (C***H***$_3$)$_3$C-P). $^{13}C\{^1H\}$ NMR (CD_2Cl_2): 165.52 (vt, $J_{PC} = 2.8$ Hz, pyridine-***C***2,6), 142.75 (s, pyridine-***C***4), 133.67 (d, $^2J_{RhC} = 9.3$ Hz, CH$_3$***C***N), 125.06 (vt, $J_{PC} = 5.3$ Hz, pyridine-***C***3,5), 38.74 (vt, $J_{PC} = 8.1$ Hz, P***C***(CH$_3$)$_3$), 37.55 (vt, $J_{PC} = 8.0$ Hz, P***C***(CH$_3$)$_3$), 34.04 (vt, $J_{PC} = 10.2$ Hz, 2 Ar-***C***H$_2$-P), 29.97 (s, 2(***C***H$_3$)$_3$C-P), 28.47

(s, 2(***C***H_3)$_3$C-P), 4.92 (s, ***C***H_3CN) (assignment of ^{13}C{H} NMR signals was confirmed by ^{13}C DEPT135). IR ν (neat; cm^{-1}): 1710 (s, NO), 2327 (w, CH_3CN), 2298 (w, CH_3CN). IR ν (mineral oil; cm^{-1}): 1703 (s, NO), 2335 (w, CH_3CN). Anal. Calcd: C, 40.41; H, 6.24. Found: C, 40.33; H, 6.18.

X-ray Structural Analysis of 6. ***Crystal data:*** $C_{25}H_{43}N_3OP_2Rh + 1/2(C_6H_6) + 2BF_4$, blue-green, prism, 0.2 × 0.1 × 0.1 mm^3, monoclinic; *P*2(1)/*n* (#14); a = 11.705(2) Å, b = 16.359(3) Å, c = 19.271(4) Å; β = 98.26(3)°, from 20 degrees of data; T = 120(2) K; V = 3651.8(12) Å^3, Z = 4; fw = 779.15; D_c = 1.417 Mg/m^3; μ = 0.622 mm^{-1}. *Data Collection and Processing:* Nonius KappaCCD diffractometer, Mo Kα (λ = 0.71073 Å), graphite monochromator; $-15 \le h \le 15$, $0 \le k \le 21$, $0 \le l \le 24$, frame scan width = 1.0°, scan speed 1.0° per 40 s, typical peak mosaicity 0.415°, 34 348 reflections collected, 8303 independent reflections (R_{int} = 0.052). The data were processed with Denzo-Scalepack. *Solution and Refinement:* The structure was solved by direct methods with SHELXS-97. Full-matrix least-squares refinement based on F^2 with SHELXL-97; 405 parameters with 0 restraints, final R_1 = 0.0468 (based on F^2) for data with $I > 2\sigma(I)$ and R_1 = 0.0658 on 8303 reflections, goodness-of-fit on F^2 = 1.080, largest electron density peak = 2.401 e Å^{-3}.

Characterization of ^{15}N-Labeled 6. ^{15}N NMR (CD_2Cl_2, at −60 °C): 829.76 (br s). ^{31}P{^{1}H} NMR (CD_2Cl_2): 73.05 (d, $^1J_{RhP}$ = 103.9 Hz). ^{1}H NMR (CD_2Cl_2): 8.05 (t, $^3J_{HH}$ = 7.8 Hz, 1H, pyridine-***H***4), 7.93 (d, $^3J_{HH}$ = 7.9 Hz, 2H, pyridine-***H***3,5), 4.0 (AB quartet, $^2J_{HH}$ = 18.8 Hz, 4H, Ar-C***H***$_2$-P), 2.94 (s, 3H, C***H***$_3$CN), 1.32 (vt, J_{PH} = 7.3 Hz, 18H, 2 (C***H***$_3$)$_3$C-P), 1.22 (vt, J_{PH} = 8.0 Hz, 18H, 2 (C***H***$_3$)$_3$C-P). ^{13}C{^{1}H} NMR (CD_2Cl_2): 165.28 (vt, J_{PC} = 2.5 Hz, pyridine-***C***2,6), 142.33 (s, pyridine-***C***4), 133.39 (d, $^2J_{RhC}$ = 8.7 Hz, CH_3***C***N), 124.68 (vt, J_{PC} = 5.3 Hz, pyridine-***C***3,5), 38.31 (vt, J_{PC} = 8.2 Hz, P***C***(CH$_3$)$_3$), 37.05 (vt, J_{PC} = 8.2 Hz, P***C***(CH$_3$)$_3$), 33.48 (vt, J_{PC} = 10.5 Hz, 2 Ar-***C***H$_2$-P), 29.56 (s, 2(***C***H$_3$)$_3$C-P), 28.06 (s, 2(***C***H$_3$)$_3$C-P), 4.53 (s, ***C***H$_3$CN) (assignment of ^{13}C{H} NMR signals was confirmed by ^{13}C DEPT135). IR ν (mineral oil; cm^{-1}): 1671 (s, ^{15}NO), 2329 (w, CH_3CN).

Reaction of Rh(PCP′Bu)(CH$_3$)Cl (7) with NOBF$_4$. Formation of [Rh(PCP′Bu)(CH$_2$)(NO)][BF$_4$] (8) and Complex 9. A cold red solution of **7** (20 mg, 0.035 mmol) in methylene chloride (1 mL) was added to cold solid $NOBF_4$ (4.1 mg, 0.035 mmol). Immediate color change from red to dark brown took place. The solvent was evaporated and the remaining solid was washed with ether, benzene, and THF and redissolved in dichloromethane, giving 8.7 mg of **8** (44% yield). Single crystals suitable for X-ray diffraction were obtained by slow diffusion of pentane into a concentrated solution of **8** in CH_2Cl_2 at room temperature. Complex **9** was obtained as a byproduct resulting from the reaction of HCl generated during the reaction.

Characterization of 8. ^{31}P{^{1}H} NMR (CD_2Cl_2): 109.62 (d, $^1J_{RhP}$ = 153.7 Hz). ^{1}H NMR (CD_2Cl_2): 6.73 (s, 1H, Rh-***Ar***), 3.46 (td, $^3J_{PH}$ = 10.5 Hz, $^2J_{RhH}$ = 2.9 Hz, 2H, Ar-C***H***$_2$-Rh), 3.36 (vt, J_{PH} = 3.5 Hz, 4H, 2 Ar-C***H***$_2$-P), 2.28 (s, 6H, 2 Ar-C***H***$_3$), 1.54 (vt, J_{PH} = 7.0 Hz, 18H, 2 (C***H***$_3$)$_3$C-P), 1.34 (vt, J_{PH} = 7.0 Hz, 18H, 2 (C***H***$_3$)$_3$C-P). ^{13}C{^{1}H} NMR (CD_2Cl_2): 139.92 (s, Rh-***Ar***), 134.20 (vt, $^3J_{PC}$ = 3.8 Hz, Rh-***Ar***), 132.31 (s, Rh-***Ar***), 123.20 (vt, $^2J_{PC}$ = 4.6 Hz, Rh-***Ar***), 40.52 (vtd, J_{PC} = 4.6 Hz, $^2J_{RhC}$ = 1.5 Hz, (CH$_3$)$_3$***C***-P), 37.68 (vt, J_{PC} = 6.5 Hz, (CH$_3$)$_3$***C***-P), 32.47 (br dt, J_{RhC} = 19.1 Hz, J_{PC} = 2.3 Hz, Ar-***C***H$_2$-Rh), 30.21 (s, (***C***H$_3$)$_3$C-P), 29.85 (s, (***C***H$_3$)$_3$C-P), 21.29 (vt, J_{PC} = 9.9 Hz, Ar-***C***H$_2$-P), 19.68 (s, ***C***H$_3$-Ar) (assignment of ^{13}C{H} NMR signals was confirmed by ^{13}C DEPT135). IR ν (mineral oil; cm^{-1}): 1698 (s, NO). IR ν (CH_2Cl_2; cm^{-1}): 1726 (s, NO). Anal. Calcd: C, 49.48; H, 7.54. Found: C, 49.54; H, 7.42.

X-ray Structural Analysis of 8. ***Crystal data:*** $C_{27}H_{49}NOP_2Rh + BF_4$, orange, plate, 0.1 × 0.1 × 0.05 mm^3, triclinic; $P\bar{1}$; a = 8.5787(2) Å, b = 12.6713(4) Å, c = 15.3075(5) Å; α = 113.789(2)°, β = 97.889(2)°, γ = 92.405(2)°, from 15 degrees of data; T = 120(2) K; V = 1499.42(8) Å^3, Z = 2; fw = 655.33; D_c = 1.451 Mg/m^3; μ = 0.722 mm^{-1}. *Data Collection and Processing:* Nonius KappaCCD diffractometer, Mo Kα (λ = 0.71073 Å), graphite monochromator; $-10 \le h \le 10$, $-15 \le k \le 13$, $0 \le l \le 18$, frame scan width = 1.0°, scan speed 1.0° per 140 s, typical peak mosaicity 0.73°, 32 040 reflections collected, 6846 independent reflections (R_{int} = 0.090). The data were processed with Denzo-Scalepack. *Solution and Refinement:* The structure was solved by direct methods with SHELXS-97. Full-matrix least-squares refinement based on F^2 with SHELXL-97; 339 parameters with 0 restraints, final R_1 = 0.0452 (based on F^2) for data with $I > 2\sigma(I)$ and R_1 = 0.0647 on 5487 reflections, goodness-of-fit on F^2 = 1.018, largest electron density peak = 0.972 e Å^{-3}.

Characterization of ^{15}N-Labeled 8. ^{15}N NMR (CD_2Cl_2, at −60 °C): 377.06 (d, $^1J_{RhN}$ = 33.6 Hz). ^{31}P{^{1}H} NMR (CD_2Cl_2): 109.92 (d, $^1J_{RhP}$ = 153.6 Hz). ^{1}H NMR (CD_2Cl_2): 6.72 (s, 1H, Rh-***Ar***), 3.46 (td, $^3J_{PH}$ = 11.9 Hz, $^2J_{RhH}$ = 2.4 Hz, 2H, Ar-C***H***$_2$-Rh), 3.38 (vt, J_{PH} = 3.1 Hz, 4H, 2 Ar-C***H***$_2$-P), 2.28 (s, 6H, 2 Ar-C***H***$_3$), 1.54 (vt, J_{PH} = 7.0 Hz, 18H, 2 (C***H***$_3$)$_3$C-P), 1.35 (vt, J_{PH} = 7.0 Hz, 18H, 2 (C***H***$_3$)$_3$C-P). ^{13}C{^{1}H} NMR (CD_2Cl_2): 139.93 (s, Rh-***Ar***), 134.24 (vt, $^3J_{PC}$ = 3.8 Hz, Rh-***Ar***), 132.35 (s, Rh-***Ar***), 123.24 (vt, $^2J_{PC}$ = 4.5 Hz, Rh-***Ar***), 40.56 (vtd, J_{PC} = 4.7 Hz, $^2J_{RhC}$ = 1.9 Hz, (CH$_3$)$_3$***C***-P), 37.72 (vt, J_{PC} = 6.4 Hz, (CH$_3$)$_3$***C***-P), 32.49 (br dt, J_{RhC} = 19.1 Hz, J_{PC} = 3.0 Hz, Ar-***C***H$_2$-Rh), 30.24 (vt, J_{PC} = 1.9 Hz, (***C***H$_3$)$_3$C-P), 29.88 (vt, J_{PC} = 1.9 Hz, (***C***H$_3$)$_3$C-P), 21.33 (vt, J_{PC} = 10.1 Hz, Ar-***C***H$_2$-P), 19.71 (s, ***C***H$_3$-Ar) (assignment of ^{13}C{H} NMR signals was confirmed by ^{13}C DEPT135). IR ν (mineral oil; cm^{-1}): 1666 (s, ^{15}NO).

Acknowledgment. We gratefully acknowledge financial support from Fundación Antorchas and the Israel Science Foundation. D.M. is the holder of the Israel Matz Professorial Chair of Organic Chemistry.

Supporting Information Available: CIF files containing X-ray crystallographic data for **2**, **3**, **4**, **6**, and **8**. This material is available free of charge via the Internet at http://pubs.acs.org.

OM8011536